ACS OMEGA

Article

http://pubs.acs.org/journal/acsodf

Optimized Atmospheric-Pressure Chemical Vapor Deposition Thermochromic VO_2 Thin Films for *Intelligent* Window Applications

Delphine Malarde, Michael J. Powell, Raul Quesada-Cabrera, Rachel L. Wilson, Claire J. Carmalt, Gopinathan Sankar, Ivan P. Parkin, and Robert G. Palgrave*

Department of Chemistry, Materials Chemistry Centre, University College London, 20 Gordon Street, London WC1H 0AJ, U.K.

Supporting Information

ABSTRACT: Monoclinic vanadium(IV) oxide (VO_2) has been widely studied for energy-efficient glazing applications because of its thermochromic properties, displaying a large change in transmission of near-IR wavelengths between the hot and cold states. The optimization of the reaction between VCl_4 and ethyl acetate via atmospheric-pressure chemical vapor deposition (APCVD) was shown to produce thin films of monoclinic VO_2 with excellent thermochromic properties (ΔT_{sol} = 12%). The tailoring of the thermochromic and visible light transmission was shown to be possible by altering the density and morphology of the deposited films. The films were characterized by X-ray diffraction, atomic-force microscopy, scanning electron microscopy, ellipsometry, and UV−vis spectrometry. This article provides useful design rules for the synthesis of high-quality VO_2 thin films by APCVD.

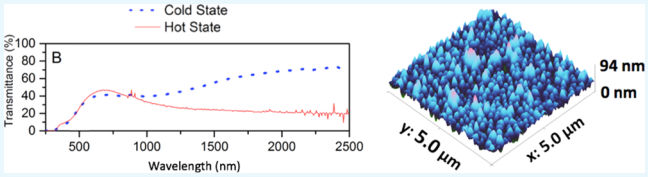

INTRODUCTION

Climate change is one of the major challenges for humankind to overcome in the near future. Over the last 40 years, a rapid increase of the average global temperature has been observed. This can be seen through the intensification of extreme weather events, melting of glaciers and sea-level rise,[1] with consequences on food and water supply, as well as human health.[2] In March 2016, it was approximately 1.5 °C above the preindustrial era average temperature.[3] This correlates with the increase of the total anthropogenic greenhouse gas emissions, which has risen by 61% during the same period.[4] In addition to finding alternative sources of energy, this has also led to a greater focus on energy efficiency and overall energy consumption. The building sector is an area that can deliver large reductions in energy consumption as it has been estimated to contribute up to a third of annual greenhouse gas emissions. This is mainly due to heating and cooling demands, as well as lighting.[5] As windows are responsible for a significant amount of the energy loss from buildings, a promising approach to improve the energy efficiency of buildings is the use of *intelligent* coatings on glazing surfaces. Thermochromic thin films are an example of one such *intelligent* coating and can play an important role in the area of energy-efficient glazing. They display a reversible change in near-infrared (NIR) reflectivity in response to temperature.[6]

Monoclinic VO_2 has been widely studied for energy-efficient glazing applications because of its thermochromic properties. At the critical temperature (T_c) of ca. 68 °C, a reversible metal-to-semiconductor transition (MST) occurs.[7] That is, from the semiconducting monoclinic phase (VO_2(M)) to the semimetallic rutile phase (VO_2(R)).[8] This transition involves changes in optical properties in the NIR region as well as a large change in electrical conductivity.[9] VO_2 thin films can be synthesized through different techniques such as magnetron sputtering,[10,11] pulsed laser deposition,[12] chemical vapor deposition (CVD),[13] and sol−gel processes.[14] This article reports on the use of atmospheric-pressure CVD (APCVD), which is a large-scale production process currently used to deposit functional coatings in industrial processes (e.g., self-cleaning coating Pilkington Activ). For VO_2 to be used for energy-efficient glazing, visible light transmittance (T_{lum}) and solar modulation (ΔT_{sol}) are the two major parameters that need improvement. Unfortunately, optimizing both T_{lum} and ΔT_{sol} in the same film has proven challenging, with thin films displaying high visible light transmission but poor solar modulation and thick films displaying the opposite trend. Optical models have been designed for improving thermochromic properties of VO_2. These models have shown that the ideal thickness should be between 60 and 100 nm to keep an acceptable visible light transmittance while maintaining reasonable solar modulation values.[15] The density of the deposited films is also an important consideration. Films with a high density can show better ΔT_{sol} because of a higher electron mobility and also present fewer defects, resulting in a decrease of incident light scattering and a higher $T_{lum.}$[16] Both the growth rate and film density may be influenced by having a fine control over the temperature and flow rate of the precursors in APCVD. This is particularly achievable when using highly volatile precursors, and their selection is thus crucial for a high performance of thermochromic coatings.

Several precursors have been used for the growth of VO_2 thin films on glass substrates via APCVD. $VOCl_3$ has been shown to

Received: January 12, 2017
Accepted: February 17, 2017
Published: March 20, 2017

DOI: 10.1021/acsomega.7b00042
ACS Omega 2017, 2, 1040−1046

produce monoclinic VO_2 when reacted with water. However, this process requires high reactor temperatures (above 600 °C). Below this temperature, or with an excess of $VOCl_3$, undesirable V_2O_5 is produced.[17] $VO(iOPr)_3$ has been used as a single precursor in APCVD.[18] Although it lowers the deposition temperature required to achieve monoclinic VO_2 (450 °C), the slow growth rate of 8 nm min^{-1} is not convenient for large-scale processes. A number of studies also related $VO(acac)_2$ and VCl_4 as precursors for growing VO_2 thin films by reaction with water.[14] A comparative study[9] investigated both precursors for depositing thin films of VO_2 by APCVD. These authors found that the films deposited from $VO(acac)_2$ showed a greater change in NIR reflectivity between the hot and cold states. However, deposition with $VO(acac)_2$ is a complex system, which may lead to undesired byproducts. In addition, it is not a convenient precursor for APCVD because of its low vapor pressure. VCl_4 was found to be a suitable simple precursor with a relatively high vapor pressure. However, so far, the deposition of VO_2 films from VCl_4 has been carried out using water as the oxygen source. VCl_4 is highly reactive with water, resulting in inhomogeneous or highly porous VO_2 films, which may have an impact on the optical properties of the deposited films.[19] In the current work, the synthesis of homogeneous thermochromic VO_2 thin films was carried out from VCl_4 and ethyl acetate (EtAc) using APCVD. We show here that EtAc is an excellent oxygen precursor because of its high vapor pressure and clean reaction with VCl_4, resulting in the formation of smooth, homogeneous thin films. The VCl_4/EtAc system was optimized, allowing for precise control over both the film growth rate and porosity of the deposited films. This research is an important step toward the development of high-performance thermochromic coatings from APCVD processes.

RESULTS AND DISCUSSION

Thin Film Synthesis and Characterization. Monoclinic VO_2 thin films were deposited onto floating glass substrates via APCVD from the reaction between VCl_4 and EtAc. The molar flow ratio was 2:1, VCl_4/EtAc, and the deposition temperature was kept constant at 550 °C. Below this temperature, the resulting VO_2 films showed high carbon contamination and were poorly crystalline, which had a drastic impact on their thermochromic properties. Nitrogen was introduced into the mixing chamber via heated stainless steel pipes, called the plain line. The total volume flow rate of the plain line was fixed at 23.2 L min^{-1}. This flow rate was found to be critical in our system: a higher flow rate (24.9 L min^{-1}) led to non-homogeneous films, whereas a lower one (21.6 L min^{-1}) produced films with poor surface coverage and poor solar modulation. Considering this, a series of four samples of VO_2(M) were synthesized under different deposition times and molar flow rates, as shown Table 1. All of the samples synthesized had a gold-brown color and passed the Scotch tape test. The films were stored in air and showed good stability over a period of several months (as assessed by UV−vis). They were also resistant to common solvents such as acetone, methanol, and ethanol.

X-ray diffraction (XRD) analysis confirmed the presence of monoclinic VO_2 phase, with preferential orientation along the (011) plane (Figure 1). Sample D showed weak diffraction peaks compared to those of the other films. As both samples B and D had comparable thicknesses, the poorly defined pattern

Table 1. Synthesis Conditions, Given as Volume Flow Rate (ϕ; Units, L min^{-1}), Molar Flow Rate (μ; Units, mol min^{-1}), Deposition Time (t; Units, min), and Thickness of VO_2 Thin Films (Determined by Ellipsometry)[a]

	T (°C)		ϕ (L min^{-1})		μ (mol min^{-1})/10^{-3}			
sample	VCl_4	EtAc	VCl_4	EtAc	EtAc	VCl_4	t (min)	thickness (nm)
A	80	40	0.8	0.2	5	3	1	177
B	80	40	0.8	0.2	5	3	0.5	65
C	40	30	0.8	0.06	1	0.5	2	125
D	40	30	0.8	0.06	1	0.5	1	72

[a]Reactor temperature was set at 550 °C. All of the depositions were carried out under a total volume flow rate of nitrogen of 23.2 L min^{-1}.

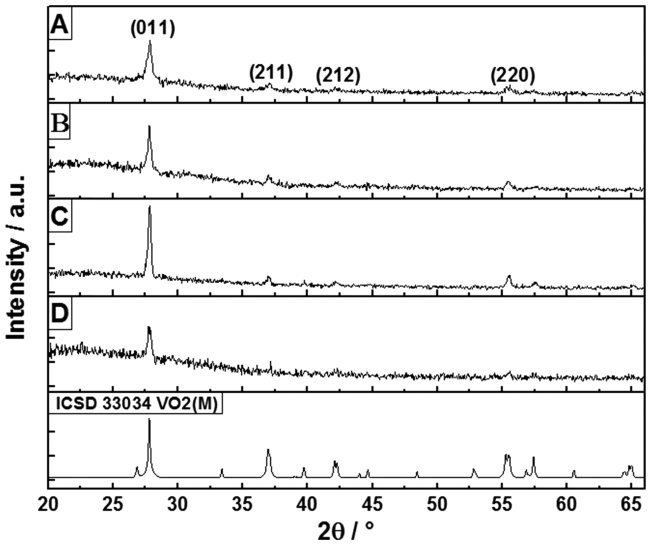

Figure 1. XRD patterns of single VO_2 films of different thicknesses: (A) 177, (B) 65.5, (C) 124.6, and (D) 72.2 nm.

of sample D suggests that it had comparatively poor crystallinity.

The chemical environments and oxidation state of vanadium were investigated by XPS. The $V2p_{3/2}$ core-level peak (Figure 2) showed the presence of two oxidation states of vanadium at

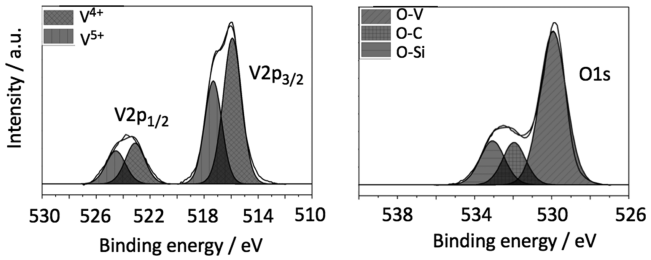

Figure 2. X-ray photoelectron spectroscopy (XPS) spectra of VO_2 thin films. The V^{4+}/V^{5+} ratio at surface thin films was 60:40.

the surface, V^{4+} and V^{5+}, at the binding energies of 515.9 and 517.3 eV, respectively. The VO_2 thin films showed a slight oxidation (presence of V_2O_5) at the extreme surface (few nanometers) because of the direct contact of the thin films with air (XPS analysis was carried out on samples stored for several months in air at room temperature). However, compared to the

DOI: 10.1021/acsomega.7b00042
ACS Omega 2017, 2, 1040−1046

films prepared previously using APCVD, those presented in this study showed a greater proportion of V^{4+} at the surface as the major contribution to the $V2p_{3/2}$ peak was from V^{4+} (V^{4+}/V^{5+} ratio was 60:40). This highlighted the good chemical stability of the VO_2 thin films. Although in situ Ar ion etching is often used to remove surface layers, it is known to cause significant changes in the vanadium oxidation state in vanadium oxides.[21] Therefore, etching cannot be used here to measure the bulk vanadium oxidation state. The binding energies at 529.9 eV in O1s signal were attributed to V—O bonds. The O1s spectra also showed the presence of carbon (C—O bonds) at the binding energy of 531.9 eV. This is likely due to the use of EtAc as the oxygen source. Finally, the binding energy of 533.3 eV was assigned to Si—O bonds. The silicon came from the SiO_2 barrier layer, suggesting the presence of pinholes into the thin films. These binding energies are in accordance with those reported in the literature.[22,23]

The surface morphology and microstructure of the films were characterized by SEM and atomic-force microscopy (AFM). SEM images of the samples displayed a uniform morphology with high surface coverage (Figure 3). However, the micro-

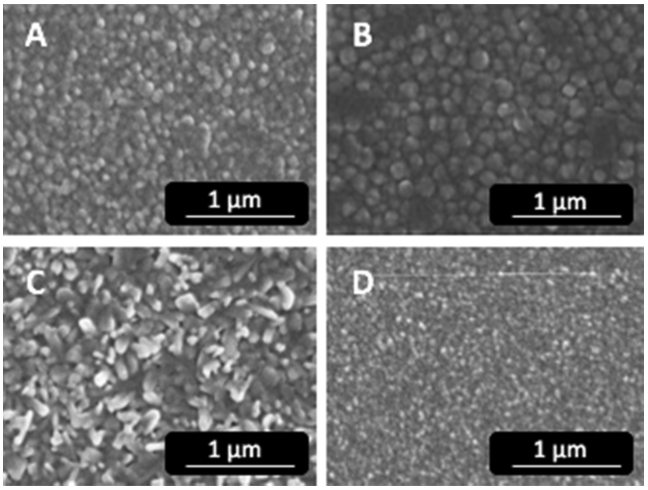

Figure 3. Scanning electron microscopy (SEM) images for a single VO_2 layer of (A) 177, (B) 65, (C) 124, and (D) 72 nm.

structure of the films was clearly different as function of the molar flow rate (μ). Samples A and B, deposited at relatively high molar flow rates ($\mu_{VCl_4} = 5 \times 10^{-3}$ mol min^{-1} and $\mu_{EtAc} = 3 \times 10^{-3}$ mol min^{-1}), showed agglomerated round particles, whereas low molar flow rates ($\mu_{VCl_4} = 1 \times 10^{-3}$ mol min^{-1} and $\mu_{EtAc} = 0.5 \times 10^{-3}$ mol min^{-1}) produced elongated particles, as seen in samples C and D. The particle growth in the four films was inferred from the different molar flow regimes used. We found that the particle sizes were comparable within short deposition times (0.5−1 min) under the high flow regime (samples A and B). However, in the low molar flow regime, there was a clear difference between the samples deposited at 1 (sample D) and 2 min (sample C), with particles in sample D being significantly smaller, likely due to the lack of available precursor.

Further morphology analysis was carried out using AFM. The three-dimensional (3D) AFM study (Figure 4) of the four VO_2 films correlated well with the SEM observations. The average surface roughness (root-mean-square, RMS) increased upon increasing the thickness of the films. This suggests that

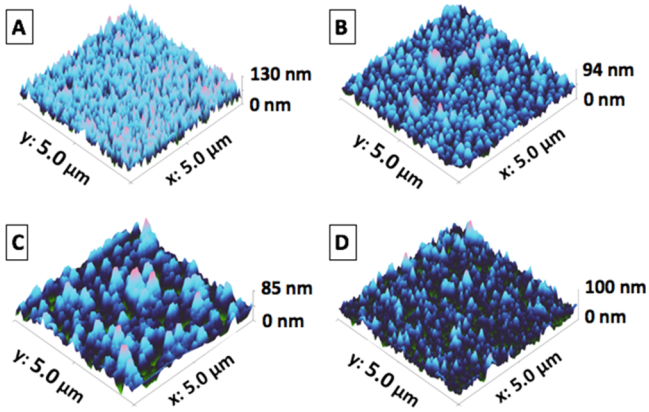

Figure 4. AFM images of the four VO_2 coatings on glass substrates. The corresponding film thicknesses were as follows: (A) 177, (B) 65, (C) 124, and (D) 72 nm for samples A−D, respectively (determined by ellipsometry).

the surface roughness of a deposited film can be tailored by controlling the molar flow rate and deposition time within the flow-rate regimes used in this work. Sample A showed significant roughness (R_{RMS} = 22 nm) compared to that of the other films (Table 2). Instead, samples B and D showed

Table 2. Average Surface Roughness of the VO_2 Films As Estimated from AFM Analysis[a]

sample	A	B	C	D
thickness (nm)	177	65.5	124.6	72.2
average RMS (nm)	22	11	14	11

[a]Films were deposited as indicated in Table 1, with film thicknesses as estimated from ellipsometry measurements.

relatively smooth surfaces with average roughness similar to that of a single VO_2 layer of 125 nm deposited by magnetron sputtering ($R_{RMS} \sim 12$ nm).[24]

Thermochromic Properties of the Optimized VO_2 Films. The thermochromic and optical properties of the VO_2 thin films were measured by recording the transmittance spectra in the UV−vis−IR regions in the range of 20−90 °C (Figure 5). All samples showed a reversible switch occurring at ∼68 °C, which is the typical temperature shown for undoped VO_2. The data from each spectrum was used to calculate the solar modulation of each sample (Table 3). For all samples, the solar modulation (T_{sol}) and the integral luminous transmittance (T_{lum}) were obtained on the basis of the spectra measured using the following equation

$$T^{\sigma}_{lum,sol} = \frac{\int \phi_{lum,sol} T^{\sigma}(\lambda)\, d\lambda}{\int \phi_{lum,sol}(\lambda)\, d\lambda}$$

where λ is the wavelength of light, ϕ_{lum} is the weighted visible light human eye, ϕ_{sol} is the weighted solar irradiance spectrum, and T^{σ} is the transmission of the VO_2 thin film in either the hot state or the cold state.

As a first observation of Table 3, the results can be split into two categories according to the synthesis conditions.

High Molar Flow Rate Regime ($\mu_{VCl_4} = 5 \times 10^{-3}$ mol min^{-1} and $\mu_{EtAc} = 3 \times 10^{-3}$ mol min^{-1}). Samples A and B showed similar solar modulations, around 12%. They also had the same large switch (around 52%) between the cold and the

DOI: 10.1021/acsomega.7b00042
ACS Omega 2017, 2, 1040−1046

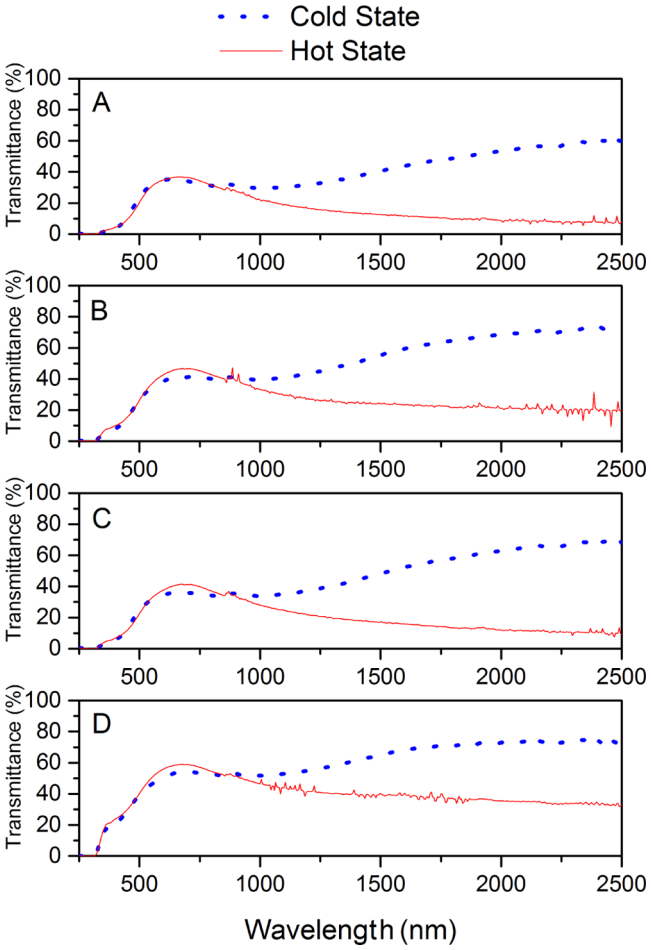

Figure 5. UV−vis spectra of the four VO_2 coatings on glass substrates. The corresponding film thicknesses were as follows: (A) 177, (B) 65, (C) 124, and (D) 72 nm for samples A−D, respectively.

Table 3. Visible Light Transmittance, T_{lum}, in the Cold State and Hot State, Total Solar Modulation, ΔT_{sol}, and Switch between the Cold and Hot States at 2500 nm

		T_{lum} (%)			
sample	thickness (nm)	cold state	hot state	ΔT_{sol} (%)	switch at 2500 nm (%)
A	177	31	30	12.0	52
C	125	31	33	11.8	58
D	72	47	51	7.8	41
B	65	35	37	11.1	52

hot state at 2500 nm. The difference between the thicknesses of samples A and B did not affect ΔT_{sol}. However, there was an impact on their visible light transmittance (T_{lum}), which was higher for the thinnest thin VO_2 film, sample B, as expected.

Low Molar Flow Rate Regime (μ_{VCl_4} = 1 × 10^{-3} mol min^{-1} and μ_{EtAc} = 0.5 × 10^{-3} mol min^{-1}). Sample C showed a ΔT_{sol} around 12%, with a large switch of 58% difference at 2500 nm. Sample D presented a ΔT_{sol} around 7.8%, with a switch of 41% at 2500 nm. Sample D showed the smallest change in transmission in this work. However, its switch is in accordance with those reported in the literature. For instance, VO_2 thin films synthesized via APCVD using VCl_4 and water as precursors showed a switch of 35% at 2500 nm.[25] At this molar flow rate, the thickness had a negative impact on ΔT_{sol}. This could be explained by the crystallinity of sample D. XRD patterns showed low crystallinity, which could reduce the thermochromic performance. On the other hand, the thinnest thin film, sample D, showed the highest T_{lum}.

Overall, all samples showed good thermochromic properties with similar ΔT_{sol}. Although sample D had the lowest ΔT_{sol}, it still showed good thermochromic performance. All of the solar modulations estimated here (7.8−12%) are in line with those of typical VO_2 thin films synthesized using other techniques, such as magnetron sputtering or spin-coating (Table 4). The thermochromic performance, in terms of solar modulation, of films from magnetron sputtering ranged between 6 and 13.4% (Table 4).[26−30] Similarly, VO_2 thin films deposited by spin-coating showed solar modulations between 6.4 and 18.6%.[31,32] The same thin film process, APCVD, for a higher thickness, around 300 nm, showed a lower solar modulation and visible light transmission, 3.1 and 14 (cold state) and 16 (hot state), respectively.[33] Also, it is important to keep in mind that optical modulations for VO_2 (finite-difference time-domain simulations) showed that the highest solar modulation reached for a single VO_2 layer synthesized by APCVD was $\Delta T_{sol} \sim 15\%$;[15] thus, our system is close to the theoretical limits.

For comparison, several data from the literature were gathered in Table 4. They showed the thermochromic properties of VO_2 thin films deposited by various methods.

Visible light transmission was dependent on film thickness for samples deposited using the same molar flow rates. This can be seen when comparing samples A and B, where upon increasing thickness, the visible light transmission decreased. For a better overview of visible light transmittance, an illustration of sample B is shown in Figure 6 and compared with a commercial window. However, this was not the case when comparing the samples deposited using different molar flow rates but with similar thicknesses, such as B (65 nm) and D (72 nm). Here, it appeared that sample D had a better T_{lum} despite being thicker than sample B. The AFM data showed similar RMS for both samples (Table 2). However, the 3D AFM scans and SEM images showed difference between the morphologies of the two samples. Sample D had more elongated particle shapes and a less compact surface. Although they had similar thicknesses, the average size of the particles for these two samples was very different. Sample B had an average particle size of ca. 143 nm, whereas sample D showed average particle size of ca. 30 nm. Zhou et al.[34] demonstrated that for VO_2 particle sizes below 50 nm the light scattering was very weak, with visible wavelengths only interacting poorly with the VO_2 particles. This resulted in higher visible light transmission. Conversely, the light scattering increased with particle size. Therefore, the higher visible light transmittance observed in sample D could be due to a weaker light scattering than that for sample B.

As a result, VO_2 thin film with a certain thickness and morphology (sample D) was obtained. The sample displayed a high visible light transmittance, 47 and 51% in cold and hot states, respectively, while maintaining a good solar modulation. As seen in Table 4, T_{lum} of sample D is higher than T_{lum} of VO_2 thin films deposited by magnetron sputtering, with similar ΔT_{sol}. Magnetron sputtering is an expensive thin film deposition process that requires low pressure and low growth rate. Considering this, this article showed the experimental conditions to synthesize VO_2 thin films that displayed good thermochromic properties and high visible light transmittance with a cheaper thin film deposition technique (APCVD) and

DOI: 10.1021/acsomega.7b00042
ACS Omega 2017, 2, 1040−1046

Table 4. Thermochromic Properties of Different VO_2 Thin Films as a Function of the Deposition Process

method	sample	thickness (nm)	T_{lum} cold state (%)	T_{lum} hot state (%)	ΔT_{sol} (%)	ref
magnetron sputtering	VO_2	90	38	38	6.0	26
	VO_2 thin film on MgF_2 (111) substrate	120	41.7	33.9	11.2	27
	VO_2	50	42	45	4.5	28
	VO_2/SiO_2/glass		27.6	26.3	6.3	29
	VO_2/quartz glass	55	34.1	35.3	6.8	30
spin-coating	VO_2	119	38.4	40.4	9.7	31
polymer-assisted deposition	VO_2	102	43.3	39.9	14.1	32
APCVD	VO_2	300	14.1	16.5	3.1	33
	VO_2/glass (A)	177	31	30	12.0	[a]
	VO_2/glass (C)	125	31	33	11.8	[a]
	VO_2/glass (D)	72	47	51	7.8	[a]
	VO_2/glass (B)	65	35	37	11.1	[a]

[a]This work.

Figure 6. Evaluation of visible transmittance through a typical VO_2 film (sample B, thickness 72 nm) deposited on glass showing the outside view. The photographs of the outside view were taken without (left) and with (right) the VO_2 coating. Photograph courtesy of Delphine Malarde. Copyright 2016.

commercial precursors and at a fast growth rate. Although the visible light transmittance was high for a single VO_2 layer, a higher T_{lum} for samples A−C is required to meet the standards of window and glazing markets. It is important to note that commercial windows are often sold with a visible light transmittance of 45−55%. For instance, anti-reflection (AR) layers could be grown on the top of VO_2 thin films for improving T_{lum}. This could be the subject of a future study.

CONCLUSIONS

Single-layer VO_2 thin films were synthesized by APCVD using VCl_4 and EtAc as vanadium and oxygen precursors, respectively. It has been found that EtAc is a convenient oxygen source to use in APCVD and can be used with VCl_4 to synthesize VO_2 thin films. The use of EtAc allowed us to finely control film morphology and thickness as a function of the molar flow rate and deposition time. This study proposes the experimental conditions to grow high-quality VO_2 thin films with commercial precursors and high growth rates, which is an advantage for large-scale processes. The VO_2 films showed excellent thermochromic properties (ΔT_{sol} = 7.8−12%) and were highly reproducible. The visible light transmission of the VO_2 thin films discussed in this work is among the highest for thin films deposited by APCVD processes. However, these values could be further improved upon addition of AR coatings and nanostructuring of the films.

EXPERIMENTAL SECTION

All chemicals were purchased from Sigma-Aldrich. Vanadium(IV) chloride (VCl_4, 99%) and EtAc ($C_4H_8O_2$, 99.8%) were used as the V and O sources, respectively. The substrate was float glass (15 × 7 cm^2; Pilkington, United Kingdom), coated with a SiO_2 barrier layer (50 nm). The deposition occurred on the barrier coating, which was identified using a UVC lamp (λ = 254 nm). Prior to deposition, substrates were cleaned with soap, acetone, isopropan-2-ol, and deionized water and left to air-dry.

APCVD. All of the experiments were performed on a custom-built APCVD rig. The rig consisted of two bubblers, containing precursors, which were linked to the reactor and the exhaust via heated stainless steel pipes, as shown Figure 7. The

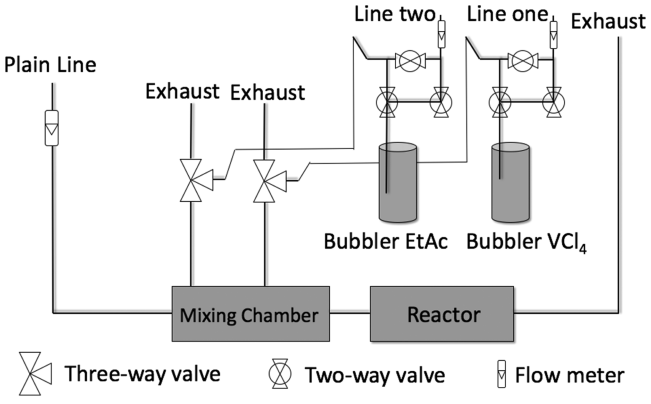

Figure 7. APCVD rig scheme.

reactor consisted of a quartz tube with a carbon block with three inserted *Whatman* heater cartridges. All heaters were controlled by Eurotherm controllers and RS type-k thermocouples. The bubblers were heated so as to produce enough vapor pressure from the precursors. The vaporized precursors were then carried to the reaction chamber by a flow of oxygen-free N_2 (BOC). The mass flow of the precursors, VCl_4 and EtAc, into the reactor was calculated from the equation below

$$a = \frac{V_p \times F}{(760 - V_p) \times 24.4}$$

DOI: 10.1021/acsomega.7b00042
ACS Omega 2017, 2, 1040−1046

where a is the amount of material introduced (in mol min^{-1}), V_p is the vapor pressure of the material at the temperature in the bubbler (mmHg), F is the flow rate of the carrier gas (L min^{-1}). Once the deposition was complete, the substrate would be left to cool under a flow of N_2 before being removed once below 80 °C. All samples were handled and stored in air.

Film Analysis. The surface morphologies of the films were determined by SEM using a JEOL JSM-6700 microscope (3 kV). The roughness measurements were obtained using a Nanosurf easy scan AFM, equipped with a 10 μm tip in noncontact mode with an oscillating probe. The scan area was 5 μm × 5 μm with 20 nm scan intervals. XRD was performed on a Bruker D8 Discover LynxEye diffractometer using primary monochromated Cu Kα_1 radiation (λ = 1.5406 Å, 2θ = 5−66°, 0.05° per step). XRD patterns were compared with Inorganic Crystal Structure Database (ICSD) reference patterns for monoclinic VO_2 (ICSD 34033). Optical transmittances were monitored on a Perkin Elmer Lambda 950 UV−vis−NIR spectrophotometer that was equipped with a homemade heating unit. The thermochromic properties of the films were measured by recording the transmittance spectra from 2500 to 250 nm as a function of temperature between 20 and 90 °C. The Scotch tape test[20] was used to determine the adhesion of the films to the substrate. Thin films thicknesses were determined by the φ SemiLab SE-2000 ellipsometer. XPS was carried out on thin films using a Thermo Scientific K-α spectrometer with monochromated Al Kα radiation, a dual beam charge compensation system, and constant pass energy of 50 eV (spot size, 400 μm). Spectra were recorded from 0 to1200 eV.

■ ASSOCIATED CONTENT

Supporting Information

The Supporting Information is available free of charge on the ACS Publications website at DOI: 10.1021/acsomega.7b00042.

Reversibility of the thermochromic thin films, UV−vis spectra, relevant details about XRD patterns and crystallinity of thin films (PDF)

■ AUTHOR INFORMATION

Corresponding Author

*E-mail: r.palgrave@ucl.ac.uk.

ORCID

Delphine Malarde: 0000-0001-7797-7686

Claire J. Carmalt: 0000-0003-1788-6971

Gopinathan Sankar: 0000-0001-5152-3424

Notes

The authors declare no competing financial interest.

■ ACKNOWLEDGMENTS

This study was funded by the chemistry department of UCL and the Engineering and Physical Sciences Research Council, EPSRC (EP/M003353/1 intelligent coatings for energy-efficient glazing, ICE glazing). Dr. Alaric Taylor is thanked for his help with ellipsometry measurements.

■ REFERENCES

(1) Schneider, S. H. The Greenhouse Effect: Science and <tep-common:author-query>AQ6: Please check whether the updated information in ref 1 is correct.</tep-common:author-query>Policy. *Science* **1989**, *243*, 771−781.

(2) McMichael, A. J.; Woodruff, E.; Hales, S. Climate Change and Human Health: Present and Future Risks. *Lancet* **2006**, 859−869.

(3) Morice, C. P.; Kennedy, J. J.; Rayner, N. A.; Jones, P. D. Quantifying Uncertainties in Global and Regional Temperature Change Using an Ensemble of Observational Estimates: The HadCRUT4 Data Set. *J. Geophys. Res.: Atmos.* **2012**, *117*, 1−22.

(4) IPCC. *Summary for Policymakers*, 2014.

(5) Lemmet, S. *Buildings and Climate Change*; UNEP, 2013.

(6) Li, S.-Y.; Niklasson, G. A.; Granqvist, C. G. Nanothermochromics with VO_2 Based Core Shell Structures: Calculated Luminous and Solar Optical Properties. *J. Appl. Phys.* **2011**, *109*, No. 113515.

(7) Granqvist, C. G.; Green, S.; Niklasson, G. A.; Mlyuka, N. R.; von Kræmer, S.; Georén, P. Advances in Chromogenic Materials and Devices. *Thin Solid Films* **2010**, *518*, 3046−3053.

(8) Zhang, Z.; Gao, Y.; Chen, Z.; Du, J.; Cao, C.; Kang, L.; Luo, H. Thermochromic VO_2 Thin Films: Solution-Based Processing, Improved Optical Properties, and Lowered Phase Transformation Temperature. *Langmuir* **2010**, *26*, 10738−10744.

(9) Vernardou, D.; Pemble, M. E.; Sheel, D. W. The Growth of Thermochromic VO_2 Films on Glass by Atmospheric-Pressure CVD: A Comparative Study of Precursors, CVD Methodology, and Substrates. *Chem. Vap. Deposition* **2006**, *12*, 263−274.

(10) Zhang, D. P.; Zhu, M. D.; Liu, Y.; Yang, K.; Liang, G. X.; Zheng, Z. H.; Cai, X. M.; Fan, P. High Performance VO2 Thin Films Growth by DC Magnetron Sputtering at Low Temperature for Smart Energy Efficient Window Application. *J. Alloys Compd.* **2016**, *659*, 198−202.

(11) Luo, Y. Y.; Pan, S. S.; Xu, S. C.; Zhong, L.; Wang, H.; Li, G. H. Influence of Sputtering Power on the Phase Transition Performance of VO_2 Thin Films Grown by Magnetron Sputtering. *J. Alloys Compd.* **2016**, *664*, 626−631.

(12) Koo, H.; Shin, D.; Bae, S. H.; Ko, K. E.; Chang, S. H.; Park, C. The Effect of CeO_2 Antireflection Layer on the Optical Properties of Thermochromic VO_2 Film for Smart Window System. *J. Mater. Eng. Perform.* **2014**, *23*, 402−407.

(13) Vernardou, D.; Louloudakis, D.; Spanakis, E.; Katsarakis, N.; Koudoumas, E. Functional Properties of APVCD VO_2 Layers. *Int. J. Thin Films Sci. Technol.* **2015**, *4*, 187−191, DOI: 10.12785/ijtfst/040305.

(14) Hu, Y.; Shi, Q.; Huang, W.; Zhu, H.; Yue, F.; Xiao, Y.; Liang, S.; Lu, T. Preparation and Phase Transition Properties of Ti Doped VO_2 Films by Sol Gel Process. *J. Sol-Gel Sci. Technol.* **2016**, *78*, 19−25.

(15) Taylor, A.; Parkin, I.; Noor, N.; Tummeltshammer, C.; Brown, M. S.; Papakonstantinou, I. A Bioinspired Solution for Spectrally Selective Thermochromic VO_2 Coated Intelligent Glazing. *Opt. Express* **2013**, *21*, A750−A764.

(16) Li, Y.; Liu, Y.; Liu, J.; Ren, L. The Effects of Niobium on the Structure and Properties of VO_2 Films. *J. Mater. Sci.: Mater. Electron.* **2016**, *27*, 4981−4987.

(17) Manning, T. D.; Parkin, I. P. Vanadium(IV) Oxide Thin Films on Glass and Silicon from the Atmospheric Pressure Chemical Vapour Deposition Reaction of $VOCl_3$ and Water. *Polyhedron* **2004**, *23*, 3087−3095.

(18) Papadimitropoulos, G.; Kostis, I.; Trantalidis, S.; Tsiatouras, A.; Vasilopoulou, M.; Davazoglou, D. *Phys. Status Solidi* **2015**, *12*, 964−968.

(19) Béteille, F.; Mazerolles, L.; Livage, J. Microstructure and Metal-Insulating Transition of VO_2 Thin Films. *Mater. Res. Bull.* **1999**, *34*, 2177−2184.

(20) Griffith, J. E.; Qiu, Y.; Tombrello, T. A. Ion Beam Enhanced Adhesion in the Electronic Stopping Region. *Nucl. Instrum. Methods Phys. Res.* **1982**, *198*, 607−609.

(21) Hryha, E.; Rutqvist, E.; Nyborg, L. Stoichiometric Vanadium Oxides Studied by XPS. *Surf. Interface Anal.* **2012**, *44*, 1022−1025.

(22) Silversmit, G.; Depla, D.; Poelman, H.; Marin, G. B.; Gryse, R. De Determination of the V2p XPS Binding Energies for Different Vanadium Oxidation States (V^{5+} to V^0). *J. Electron Spectrosc. Relat. Phenom.* **2004**, *135*, 167−175.

DOI: 10.1021/acsomega.7b00042
ACS Omega 2017, 2, 1040−1046

(23) Shibata, H.; Kimura, S.; Takatoh, H. Deposition of SiO_2 Thin Films by Combined Low Energy Ion Beam and Molecular Beam Epitaxial Method. *Jpn. J. Appl. Phys.* **2000**, *39*, 1327−1328.
(24) Guinneton, F.; Sauques, L.; Valmalette, J. C.; Cros, F.; Gavarri, J. R. Optimized Infrared Switching Properties in Thermochromic Vanadium Dioxide Thin Films: Role of Deposition Process and Microstructure. *Thin Solid Films* **2004**, *446*, 287−295.
(25) Blackman, C. S.; Piccirillo, C.; Binions, R.; Parkin, I. P. Atmospheric Pressure Chemical Vapour Deposition of Thermochromic Tungsten Doped Vanadium Dioxide Thin Films for Use in Architectural Glazing. *Thin Solid Films* **2009**, *517*, 4565−4570.
(26) Mlyuka, N. R.; Niklasson, G. A.; Granqvist, C. G. Thermochromic VO_2-Based Multilayer Films with Enhanced Luminous Transmittance and Solar Modulation. *Phys. Status Solidi A* **2009**, *206*, 2155−2160.
(27) Zhou, H.; Li, J.; Xin, Y.; Sun, G.; Bao, S.; Jin, P. Optical and Electrical Switching Properties of VO_2 Thin Film on MgF_2 (111) Substrate. *Ceram. Int.* **2016**, *42*, 7655−7663.
(28) Mlyuka, N. R.; Niklasson, G. A.; Granqvist, C. G. Thermochromic Multilayer Films of VO_2 and TiO_2 with Enhanced Transmittance. *Sol. Energy Mater. Sol. Cells* **2009**, *93*, 1685−1687.
(29) Zhu, B.; Tao, H.; Zhao, X. Effect of Buffer Layer on Thermochromic Performances of VO_2 Films Fabricated by Magnetron Sputtering. *Infrared Phys. Technol.* **2016**, *75*, 22−25.
(30) Zhao, X. L.; Zhang, Y. Z.; Cao, Y. Z.; Yan, L.; Wang, X. Thermochromic Properties of VO_2 Films Deposited on Quartz Glass. *Adv. Mater. Res.* **2013**, *734*−*737*, 2420−2425.
(31) Zhang, J.; Tian, H.; Hao, L.; Jin, X.; Yang, C.; Wang, J.; Cui, X.; Wang, C.; Zhang, C.; Zhang, C.; et al. Thermochromic VO_2 Films from Ammonium Citrato-Oxovanadate(IV) with Excellent Optical and Phase Transition Properties. *J. Mater. Chem. C* **2016**, *4*, 5281−5288.
(32) Kang, L.; Gao, Y.; Luo, H.; Chen, Z.; Du, J.; Zhang, Z. Nanoporous Thermochromic VO_2 Films with Low Optical Constants, Enhanced Luminous Transmittance and Thermochromic Properties. *ACS Appl. Mater. Interfaces* **2011**, *3*, 135−138.
(33) Powell, M. J.; Quesada-Cabrera, R.; Taylor, A.; Teixeira, D.; Papakonstantinou, I.; Palgrave, R. G.; Sankar, G.; Parkin, I. P. Intelligent Multifunctional $VO_2/SiO_2/TiO_2$ Coatings for Self-Cleaning, Energy-Saving Window Panels. *Chem. Mater.* **2016**, *28*, 1369−1376.
(34) Zhou, J.; Gao, Y.; Zhang, Z.; Luo, H.; Cao, C.; Chen, Z.; Dai, L.; Liu, X. VO_2 Thermochromic Smart Window for Energy Savings and Generation. *Sci. Rep.* **2013**, *3*, No. 3029.

DOI: 10.1021/acsomega.7b00042
ACS Omega 2017, 2, 1040−1046